

Low-energy electron spectrum in copper oxides in the multiband $p-d$ model

V. A. Gavrichkov and S. G. Ovchinnikov

*L. V. Kirenskiĭ Institute of Physics, Siberian Branch of the Russian Academy of Sciences,
660036 Krasnoyarsk, Russia*

(Submitted March 25, 1997; resubmitted July 8, 1997)

Fiz. Tverd. Tela (St. Petersburg) **40**, 184–190 (February 1998)

An exact diagonalization of the Hamiltonian in the $p-d$ model of a CuO_6 cluster was used to obtain dependences on the model parameters of the lowest-energy two-hole terms: the

energy difference between the $2p$ orbitals of planar and apical oxygen

$\Delta(\text{apex}) = \varepsilon(2p) - \varepsilon[2p(\text{apex})]$, the crystal field parameter $\Delta_d = \varepsilon_{3z^2-r^2} - \varepsilon_{x^2-y^2}$, and the ratio

of the distances between the copper atom and the apical and planar oxygen atoms

$d(\text{apex})/d(\text{pl})$. In the limit of large $d(\text{apex})/d(\text{pl})$ and Δ_d , our model is equivalent to the three-

band $p-d$ model and, in this case, large singlet-triplet splitting $\Delta\varepsilon \geq 1$ eV is also observed.

As the parameters decrease, a singlet-triplet crossover is observed. Two mechanisms are identified

for stabilization of the triplet term ${}^3B_{1g}(0)$ as the ground state. It is shown that for realistic

values of the parameters, reduction of the $p-d$ model to the three-band model is limited by the low

energies of the current excitations because of the presence of the lower excited ${}^3B_{1g}$ and

${}^1A_{1g}$ cluster states. Intercluster hopping causes strong mixing of singlet and triplet states far from

the Γ point. The results of the calculations are compared with data obtained by angle-

resolved photoelectron emission in $\text{Sr}_2\text{CuO}_2\text{Cl}_2$. © 1998 American Institute of Physics.

[S1063-7834(98)00202-0]

The electronic structure of undoped and weakly-doped copper oxides does not lend itself to *ab initio* band calculations because of the difficulties involved in allowing for the strong electron correlations. The three-band $p-d$ model^{1,2} is the simplest model for the energy structure of copper oxides which takes account of strong correlation effects at the Cu cation and the ionic nature of the chemical bond of the insulating ground state of undoped oxides having a semiconductor gap as a result of charge transport. It is currently assumed that holes induced by p -type doping or intrinsic nonstoichiometry are located on the oxygen and a ‘‘hole on copper+ hole on oxygen’’ pair is in the Zhang–Rice singlet state.³ It is also assumed that the first excited state of a pair of holes is 2–3 eV higher and is unrelated to the low-energy dynamics of the current carriers. This is one reason for the appearance of numerous theoretical studies concerned with reducing the $p-d$ model to the single-band Hubbard model or the $t-J$ model.^{4–6} Nevertheless, there is theoretical and experimental evidence to indicate the importance of other states, absent from the three-band $p-d$ model. For instance, polarized x-ray absorption spectroscopy (XAS)⁷ and electron energy-loss spectroscopy (EELS)⁸ show quite measurable filling of $d_{3z^2-r^2}$ orbitals in all the oxides studied. In order to give a three-band model in accordance with the observed states, its basis must also include the $d_{3z^2-r^2}$ copper state^{9,10} and the $2p[2p(\text{apex})]$ state of planar (apical) oxygen, which transform by a similar irreducible a_{1g} representation. A study of the two-hole spectrum of a CuO_6 cluster using perturbation theory^{11,12} for model parameters determined from CuO x-ray photoemission spectroscopy (XPS) reveals that the two-hole ${}^3B_{1g}$ level for La_2CuO_4 is 0.7 eV higher than the singlet ${}^1A_{1g}$ level. This value changes to zero or even becomes negative as a result of small variations in the pa-

rameters of the model. All these factors indicate the importance of $d_{3z^2-r^2}$ orbitals for the electronic structure.

Note also that *ab initio* calculations of the electronic structure of CuO_4 and CuO_6 clusters using the self-consistent field method with configurational interaction showed that a reduction in the distance from the apical oxygen leads to stabilization of the ${}^3B_{1g}$ triplet as the ground two-hole state rather than the ${}^1A_{1g}$ singlet.¹³ The small energy spacing between these states produces changes in the low-energy part of the Fermi quasiparticle spectrum.¹⁴ It was shown in Ref. 15 that strong mixing of singlet and triplet states takes place far from the Γ point.

Here we examine two problems. First, we make a multiband analysis of the validity of the three-band $p-d$ model. It was shown in similar studies^{11,12} that between the Zhang–Rice singlet and its corresponding triplet ${}^3A_{1g}$ there are various two-hole states: ${}^3B_{1g}$, ${}^1A_{1g}$, ${}^1B_{1g}$, and others. Unlike the authors of Refs. 11 and 12, we examine in detail the dependence of these multielectron terms on the model parameters, which can reveal mechanisms for their possible stabilization as ground levels and can identify the range of validity of the three-band model. To this end, we studied the ground state of two holes in a CuO_6 cluster using the exact diagonalization method, we calculated the eigenvalues and eigenvectors as functions of the crystal field parameter $\Delta_d = \varepsilon(d_{3z^2-r^2}) - \varepsilon(d_{x^2-y^2})$, the energy difference between the $2p$ orbitals of planar and apical oxygen $\Delta(\text{apex}) = \varepsilon(2p) - \varepsilon(2p(\text{apex}))$, and the ratio of the distances between the copper atom and the apical and planar oxygen atoms $d(\text{apex})/d(\text{pl})$. In the limit of large $d(\text{apex})/d(\text{pl})$ and Δ_d values, our model is equivalent to the three-band $p-d$ model, and large singlet-triplet splitting $\Delta\varepsilon \geq 1$ eV is also observed, which agrees qualitatively with Ref. 3. By varying the values of the parameters, we observe

a reduction in the singlet-triplet splitting. For realistic parameters we find $-0.5 < \Delta \varepsilon_2 < 0.5$. In practice, this implies that there is no good energy separation between the ground and first excited current states. This factor imposes some constraints on the reduction of the multiband model to the single-band Hubbard model or the t - J model.

Second, we consider the influence of singlet-triplet mixing of states by intercluster hopping on the electron dispersion law near the top of the valence band. An intercluster hop is taken into account in perturbation theory by a method¹⁴ wherein the zeroth approximation is the exact diagonalization of the clusters. The results of the calculations showed good agreement with data obtained by angle-resolved photoelectron spectroscopy (ARPES) for the antiferromagnetic dielectric $\text{Sr}_2\text{CuO}_2\text{Cl}_2$ (Ref. 16). In addition, singlet-triplet mixing by hopping indicates that a spin-exciton mechanism of superconductivity is possible.

1. EXACT DIAGONALIZATION OF A CuO_6 CLUSTER

We consider the Hamiltonian of the $2p$ electrons at oxygen and the $3d$ electrons at copper in the hole representation

$$H = H_d + H_p + H_{pd} + H_{pp}, \quad (1)$$

where

$$H_d = \sum_{\mathbf{r}} H_d(\mathbf{r}),$$

$$H_d(\mathbf{r}) = \sum_{\lambda\sigma} \left[(\varepsilon_{d\lambda} - \mu) d_{\mathbf{r}\lambda\sigma}^+ d_{\mathbf{r}\lambda\sigma} + \frac{1}{2} U_d n_{\mathbf{r}\lambda}^\sigma n_{\mathbf{r}\lambda}^{-\sigma} \right] + \sum_{\sigma\sigma'} (V_d n_{\mathbf{r}1}^\sigma n_{\mathbf{r}2}^{\sigma'} - J_d d_{\mathbf{r}1\sigma}^+ d_{\mathbf{r}1\sigma} d_{\mathbf{r}2\sigma'}^+ d_{\mathbf{r}2\sigma'}),$$

$$H_p = \sum_{\mathbf{i}} H_p(\mathbf{i}),$$

$$H_p(\mathbf{i}) = \sum_{\alpha\sigma} \left[(\varepsilon_{p\alpha} - \mu) p_{\mathbf{i}\alpha\sigma}^+ p_{\mathbf{i}\alpha\sigma} + \frac{1}{2} U_p n_{\mathbf{i}\alpha\sigma}^\sigma n_{\mathbf{i}\alpha\sigma}^{-\sigma} \right] + \sum_{\sigma\sigma'} (V_p n_{\mathbf{i}1}^\sigma n_{\mathbf{i}2}^{\sigma'} - J_p p_{\mathbf{i}1\sigma}^+ p_{\mathbf{i}1\sigma} p_{\mathbf{i}2\sigma'}^+ p_{\mathbf{i}2\sigma'}),$$

$$H_{pd} = \sum_{\langle \mathbf{i}, \mathbf{r} \rangle} H_{pd}(\mathbf{i}, \mathbf{r}),$$

$$H_{pd}(\mathbf{i}, \mathbf{r}) = \sum_{\alpha\lambda\sigma\sigma'} (T_{\lambda\alpha} p_{\mathbf{i}\alpha\sigma}^+ d_{\mathbf{r}\lambda\sigma} + V_{\lambda\sigma} n_{\mathbf{r}\lambda}^\sigma n_{\mathbf{r}\lambda}^{\sigma'} - J_{\alpha\lambda} d_{\mathbf{r}\lambda\sigma}^+ d_{\mathbf{r}\lambda\sigma} p_{\mathbf{i}\alpha\sigma}^+ p_{\mathbf{i}\alpha\sigma}),$$

$$H_{pp} = \sum_{\langle \mathbf{i}, \mathbf{j} \rangle} \sum_{\alpha\beta\sigma} (t_{\alpha\beta} p_{\mathbf{i}\alpha\sigma}^+ p_{\mathbf{j}\beta\sigma} + \text{h.c.}).$$

Here the first two terms describe the intra-atomic energies at a copper (oxygen) site with Hubbard repulsion U_d (U_p), interorbital intra-atomic Coulomb repulsion V_d (V_p), and Hund exchange interaction J_d (J_p). The indices λ and α correspond to different orbitals in the crystal field. The third term in Eq.

(1) describes interatomic p - d hopping, Coulomb V_{pd} and exchange J_{pd} interactions. The last term in Eq. (1) corresponds to a p - p hop.

We shall consider the set of $d_{x^2-y^2}$ ($\lambda=1$) and $d_{3z^2-r^2}$ ($\lambda=2$) states of copper and p_x, p_y states of oxygen as being the most important to describe the low-energy spectrum of quasiparticles in the CuO_2 layer. We shall then use the following notation and relations between the model parameters: $\delta = \varepsilon(\sigma) - \varepsilon(d_{x^2-y^2})$, $T_{d_{x^2-y^2}, \sigma} = T_{pd}$, $T_{d_{3z^2-r^2}, \sigma(\text{apex})} = \sqrt{\frac{2}{3}} T_{pd} [d(\text{pl})/d(\text{apex})]^{3.5}$, $V_{x^2-y^2, \sigma[\sigma(\text{apex})]} \approx V_{d_{3z^2-r^2}, \sigma[\sigma(\text{apex})]} = V_{pd}$, $J_{x^2-y^2, \sigma[\sigma(\text{apex})]} \approx J_{d_{3z^2-r^2}, \sigma[\sigma(\text{apex})]} = J_{pd}$, and $t_{p_x, p_y} = t_{pp}$. The index $\sigma[\sigma(\text{apex})]$ refers to symmetrized combinations of $2p$ and $2p(\text{apex})$ oxygen orbitals which form σ bonds with $3d$ orbitals of copper. The electrically neutral compound $\text{La}_{2-x}\text{Sr}_x^{2+}(\text{CuO}_4)^{-6+x}$ corresponds to $n_h = 1 + x$ holes per formula unit. Thus, for $x=0$ we have one hole per cluster and for $x \neq 0$, two-hole states make some contribution.

Exact diagonalization of the final clusters is a powerful method of studying systems with strong electron correlations and it is desirable to take a fairly large cluster to calculate the thermodynamic averages per site and the correlation functions.¹⁷ We shall confine ourselves to the smallest possible CuO_2 , CuO_4 , and CuO_6 clusters since their exact diagonalization is required only to construct a local basis which is then used for approximate calculations of the electron Green functions of an infinite CuO_2 lattice. Diagonalization of the CuO_6 cluster is performed separately in different sectors of Hilbert space with the hole numbers $n=0, 1, 2$. The vacuum sector $n=0$ corresponds to the $3d^{10}$ configuration of copper and the $2p^6$ configuration of oxygen. In the one-hole sector, the eigenvectors are the molecular orbitals of oxygen hybridized with the $3d$ states of copper. All the basis states in the two-hole sector are different combinations of configurations of the two holes over oxygen and copper states. In our case, with one orbital per oxygen site and two orbitals per copper site, we have 28 triplet states: six ${}^3B_{1g}$, one ${}^3A_{2g}$, ten 3E_u , four ${}^3A_{1g}$, two ${}^3B_{2u}$, three ${}^3A_{2u}$, two 3E_g , and 36 singlet states: ten 1E_u , eleven ${}^1A_{1g}$, seven ${}^1B_{1g}$, one ${}^1B_{2g}$, two ${}^1B_{2u}$, three ${}^1A_{2u}$, and two 1E_g per cluster. In the following calculations only the three parameters indicated above were varied and the others were set as follows: $\delta = 3.5$ eV, $T_{pd} = 1.4$ eV, $V_d = 9$ eV, $V_p = 7$ eV, $J_d = 1$ eV, $J_p = 0.6$ eV, $V_{pd} = 0.5$ eV, and $J_{pd} = 0.2$ eV.

Figures 1a–1c give the lowest energies of the competing singlet ${}^1A_{1g}(i)$ and triplet ${}^3B_{1g}(i)$ states ($i=0$ for the ground state of this symmetry and $i=1$ for the excited state) as a function of the parameters $d(\text{apex})/d(\text{pl})$, Δ_d , and $\Delta(\text{apex})$. The fraction of states equivalent to the Zhang–Rice singlet is as high as 80% in ${}^1A_{1g}(0)$ and does not depend on the values of the above parameters. Thus, it is quite logical to identify this singlet as a Zhang–Rice singlet.³ The remaining 20% are assigned to ${}^1A_{1g}$ symmetrized states of the $(d_{x^2-y^2})^2$ and $(2p)^2$ configurations. The contributions of the atomic orbitals to the other three states ${}^1A_{1g}(1)$ and ${}^3B_{1g}(i)$ vary substantially with the values of the parameters, so they cannot be identified with any specific molecular orbital having the same symmetry.

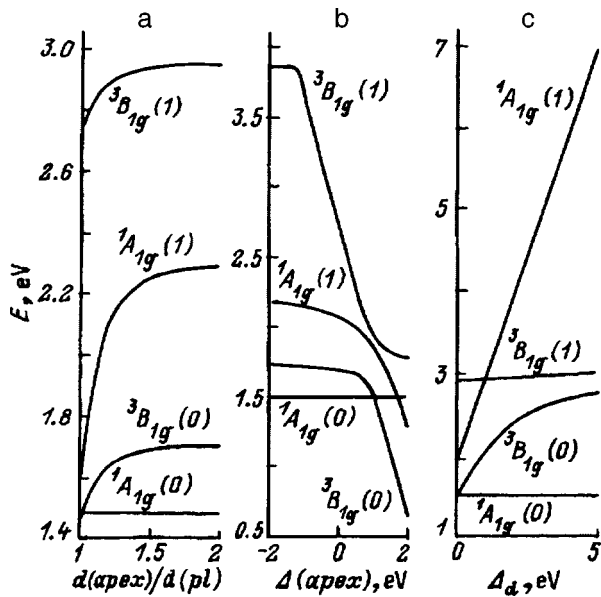


FIG. 1. Energies of the ${}^3B_{1g}(i)$ and ${}^1A_{1g}(i)$ terms as a function of the ratio of the distance between the copper atom and the apical and planar oxygen $d(\text{apex})/d(\text{pl})$ [$\Delta_d=0.3$ eV, $\Delta(\text{apex})=0.7$ eV] (a), the energy difference between the $2p$ orbitals of planar and apical oxygen $\Delta(\text{apex})=\varepsilon(2p)-\varepsilon[2p(\text{apex})](d(\text{apex})/d(\text{pl}))=1.2$, $\Delta_d=0.3$ eV (b), and the crystal field parameter $\Delta_d=\varepsilon(d_{3z^2-r^2})-\varepsilon(d_{x^2-y^2})$ [$d(\text{apex})/d(\text{pl})=1.2$, $\Delta(\text{apex})=0.7$ eV] (c).

The dependence of the level energy on $d(\text{apex})/d(\text{pl})$, plotted in Fig. 1a shows that for $d(\text{apex})/d(\text{pl}) > 1.05$ the Zhang–Rice singlet is the ground state of our cluster, which agrees well with Ref. 12, where the excited states ${}^1A_{1g}(1)$ and ${}^3B_{1g}(0)$ only extend by approximately ~ 0.2 eV above it for $d(\text{apex})/d(\text{pl}) > 1.3$. For $d(\text{apex})/d(\text{pl}) < 1.05$ the triplet ${}^3B_{1g}(0)$ becomes the ground two-hole state with the contribution made to it by the symmetrized configuration $d_{x^2-y^2}2p(\text{apex})$ increased from 10% [$d(\text{apex})/d(\text{pl})=2$] to 40% [$d(\text{apex})/d(\text{pl})=1$]. The contribution of the Hund state associated with the symmetrized configuration $d_{x^2-y^2}d_{3z^2-r^2}$ increases negligibly (to 10%).

As the energy of the $2p(\text{apex})$ orbitals of apical oxygen decreases, a crossover of the excited states and the Zhang–Rice singlet is observed (Fig. 1b). In the calculations the crossover point with the ${}^3B_{1g}$ level occurs at $\Delta(\text{apex})=1.2$ eV, which differs slightly from the 1.7 eV obtained in Ref. 11 and is attributable to differences in the calculation methods. As well as the tendency to crossover, it is observed that the fraction of the $d_{3x^2-r^2}2p(\text{apex})$ symmetrized configuration in ${}^1A_{1g}(1)$ increases from 5% [$\Delta(\text{apex})=0$] to 50% [$\Delta(\text{apex})=2$] and the fraction of the $d_{x^2-y^2}2p(\text{apex})$ -symmetrized configuration in ${}^3B_{1g}(0)$ increases from 3% to 90%. It is important to note that this is only the first of the mechanisms for stabilization of the ${}^3B_{1g}(0)$ state as the ground state and, as we can see, the $d_{x^2-y^2}2p(\text{apex})$ symmetrized configuration makes a major contribution. An increase in this contribution is observed both for this dependence and for that plotted in Fig. 1a. In both cases, we are dealing with the same stabilization mechanism. However, whereas in the first case this stabilization is associated with a decrease in the energy of the $2p(\text{apex})$

orbitals, in the second case, it is associated with the dependence of the corresponding hopping integral on the distance from the apical oxygen. As in Ref. 18, a decrease in the energy of the $2p(\text{apex})$ orbitals effectively increases their contribution to the ground two-hole state.

The ${}^3B_{1g}(0)$ and ${}^1A_{1g}(0)$ states belong to different irreducible representations and nothing prevents their crossover, but the absence of effective repulsion of the ${}^1A_{1g}(0)$ - and ${}^1A_{1g}(1)$ levels and the possible crossover of these levels appear to be a characteristic feature of our representation of the D_{4h} group. This feature is evidently closely related to the isolation of the Zhang–Rice singlet and its inability to hybridize with any states other than those of the $(d_{x^2-y^2})^2$ - and $(2p)^2$ symmetrized configurations in the absence of interactions other than H_{pd} .

A decrease in the parameter Δ_d (Fig. 1c) leads to an appreciable increase in the fraction of the Hund state and ultimately leads to convergence of the ground ${}^1A_{1g}(0)$ Zhang–Rice singlet and the excited ${}^3B_{1g}(0)$ state, particularly in the range of real values $\Delta_d \leq 1$ eV. This is the second mechanism for stabilization of the ${}^3B_{1g}$ state as the ground state. Since this mechanism involves increased Hund interaction with an increasing contribution of the $d_{x^2-y^2}d_{3z^2-r^2}$ configuration, it is more efficient as the energy of the $2p$ orbitals of planar oxygen increases and the energy of the $d_{3z^2-r^2}$ orbitals decrease. In this method of stabilizing the ${}^3B_{1g}$ state, it is observed that the fraction of $2p(\text{apex})$ states decreases whereas the fraction of the Hund configuration $d_{x^2-y^2}d_{3z^2-r^2}$ via which filling of the $d_{3z^2-r^2}$ orbitals could be observed, remains small (around 10% for $\Delta_d=0$). A similar conclusion as to the stabilizing role of the Hund exchange interaction was reached in *ab initio* calculations.¹³ It is interesting to note that a substantial decrease in the energy of the ${}^1A_{1g}(1)$ state with decreasing parameter Δ_d is associated with a negligible increase in the fraction of the $(d_{3z^2-r^2})^2$ configuration (from 5% to 15% for $\Delta_d=0$) with the major contribution being made by the $d_{3z^2-r^2}2p$ symmetrized configuration, remaining unchanged at 70%. In the “dangerous” vicinity of the ground state, we also observe the ${}^3B_{1g}(1)$ state which shows similar tendencies to converge as the parameters $d(\text{apex})/d(\text{pl})$, Δ_d , and the energy of the $2p(\text{apex})$ orbitals of apical oxygen decrease. However, because of the cluster symmetry, this level and the ${}^1B_{1g}(0)$ level repel and do not come closer than 1 eV to the ${}^1A_{1g}(0)$ level of the Zhang–Rice singlet.

2. DISCUSSION OF THE RESULTS OF THE EXACT DIAGONALIZATION

These results of the exact diagonalization of a cluster can be used to construct a local multielectron basis of states, between which hops in an infinite lattice lead to band formation. To discuss the reducibility of the p - d model to the single-band Hubbard model, we compare the more realistic local basis shown in Fig. 2a with the local basis of the Hubbard model (Fig. 2b), which consists of four states: the vacuum state $|0\rangle$, two single-particle states $|+\rangle = a_{\uparrow}^{\dagger}|0\rangle$ and $|-\rangle = a_{\downarrow}^{\dagger}|0\rangle$, and the two-particle state $|2\rangle = a_{\uparrow}^{\dagger}a_{\downarrow}^{\dagger}|0\rangle$. It can be seen from a comparison of Figs. 2a and 2b that in the energy range $E \ll \Delta\varepsilon_1$ and $E \ll \Delta\varepsilon_2$, where $\Delta\varepsilon_1$ and $\Delta\varepsilon_2$ are

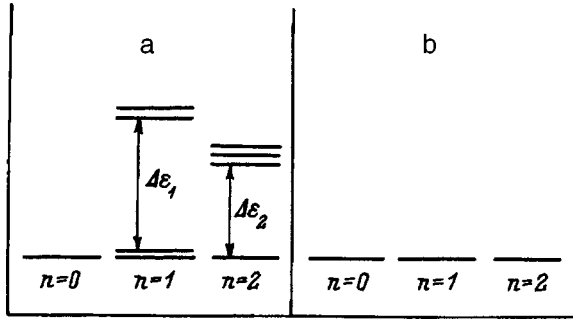


FIG. 2. Local bases of the multiband $p-d$ model (a) and the single-band Hubbard model (b). For the multiband $p-d$ model only the lowest excited terms in the single-particle and two-particle sectors of Hilbert space are shown.

the energies of the local excitations (excitons) in the single-particle and two-particle sectors of Hilbert space, the difference between the bases of the $p-d$ model and the Hubbard model can be neglected and, in this sense, it is possible to make a low-energy reduction of the $p-d$ model to the single-band Hubbard model. The single-particle exciton energy $\Delta\varepsilon_1$ is determined by the excitations in the crystal field $d_{x^2-y^2} \rightarrow d_{3z^2-r^2}$ with the energy Δ_d ; for typical parameters in copper oxides $\Delta\varepsilon_1 \geq 1$ eV. The energy of a two-particle exciton $\Delta\varepsilon_2$, associated with a hole-current carrier, depends very much on the choice of model. For instance, in the three-band $p-d$ model we find $\Delta\varepsilon_2 = 2-4$ eV and the excited triplet state can be neglected here. However, it can be seen from Figs. 1a and 1b that this situation changes in the more realistic multiband $p-d$ model where $\Delta\varepsilon_2 = E[{}^3B_{1g}(0)] - E[{}^1A_{1g}(0)]$ may be fairly small or even negative. For small $\Delta\varepsilon_2$, the range of possible reduction to the single-band model $E \leq \Delta\varepsilon_2$ becomes quite small, and for $\Delta\varepsilon_2 \leq 0$ no such range exists. Since the parameters on which $\Delta\varepsilon_2$ depends (the crystal field and the interatomic spacing) differ for different copper oxides and depend on the level of doping, it is possible to have a situation where singlet-triplet crossover takes place as the composition varies. This crossover was obtained in *ab initio* calculations¹³ for $\text{La}_{2-x}\text{Sr}_x\text{CuO}_4$ with $x \approx 0.1$; for the superconducting phase in this system the lower two-hole term is a triplet. In another model copper oxide $\text{Sr}_2\text{CuO}_2\text{Cl}_2$, an octahedron of nearest neighbors incorporates two chlorine ions along the c axis; this increases the ionicity of the Cu-Cl bond compared with Cu-O and reduces the fraction of covalent mixing of chlorine p states in the a_{1g} molecular orbital which, according to Ref. 19, is less than 1% away from the top of the valence band. It has been noted that the occupancy of the Cl p states may vary widely, without influencing the low singlet-triplet splitting energy $\Delta\varepsilon_2$. In our opinion, the smallness of $\Delta\varepsilon_2$ shows up when the dispersion law in $\text{Sr}_2\text{CuO}_2\text{Cl}_2$ measured experimentally by the ARPES method¹⁶ is compared with that calculated using the $t-J$ model.²⁰ Near the top of the valence band and in the energy range $E < 0.1$ eV, the agreement is fairly good but the differences increase for states deeper in the valence band (Fig. 3).

To calculate the dispersion law, we consider an infinite CuO_2 lattice with a unit cell in the form of an infinite cluster,

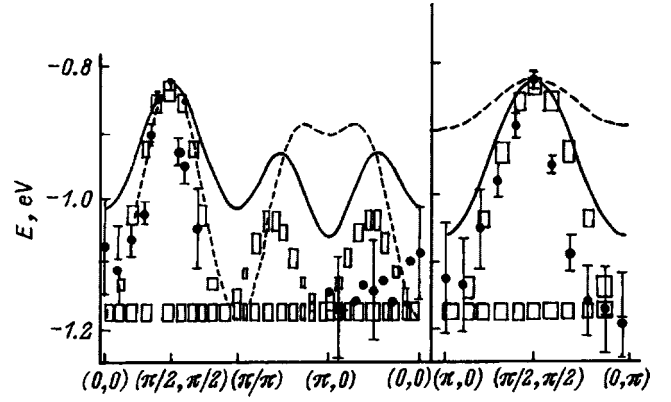


FIG. 3. Quasiparticle spectrum in $\text{Sr}_2\text{CuO}_2\text{Cl}_2$. The circles give the ARPES data,¹⁶ the dashed and solid curves give the results of calculations for the $t-J$ and $t-t'-J$ models.²⁰ The rectangles give the results of calculations using the multiband $p-d$ model.²³

for which an exact diagonalization of the initial Hamiltonian (1) has been performed. The results of the calculations are presented below.

3. DISPERSION OF ELECTRONS NEAR THE TOP OF THE VALENCE BAND

The following generalization of the strong coupling model¹⁴ is proposed to allow for the strong electron correlations within the unit cell in the band calculations: the lattice is divided into nonintersecting cells (clusters), the intracell part of the Hamiltonian is exactly diagonalized, and the eigenvectors $|p\rangle = |n, \gamma\rangle$ and terms $E_{n, \gamma}$ are found for a cluster with n particles, where the index γ numbers all the other quantum numbers. The next stage involves constructing the Hubbard operators for this cell \mathbf{f} : $X_{\mathbf{f}}^{pp'} = |n, \gamma\rangle\langle n', \gamma'|$, in whose representation the intercell component of the Hamiltonian may be written exactly as a generalized multilevel Hubbard model. As a result, the initial Hamiltonian (1) is written exactly in the form $H = H_0 + H_1$,

$$H_0 = 7 \sum_{\ln \gamma} (E_{n, \gamma} - n\mu) X_{\mathbf{f}}^{\gamma\gamma},$$

$$H_1 = \sum_{(\mathbf{f}\mathbf{g})} \sum_{\gamma\gamma'\Gamma\Gamma'} \Lambda_{\Gamma\Gamma'}^{\gamma\gamma'}(\mathbf{f}, \mathbf{g}) X_{\mathbf{f}}^{\gamma\gamma'} X_{\mathbf{g}}^{\Gamma\Gamma'}. \quad (2)$$

The spectrum of single-particle hole excitations H_0 consists of a set of dispersion-free levels (“resonances”) $\Omega_m = E_{n+1, \gamma_1} - E_{n, \gamma_2}$, where the index m is the number of possible Fermi excitations between terms $|n+1, \gamma_1\rangle \rightarrow |n, \gamma_2\rangle$. Intercluster hops described by H_1 are taken into account in perturbation theory using the simplest “Hubbard Γ ” approximation.²¹ In the double-sublattice structure of the CuO_2 layer the dispersion equation has the form

$$\det\{\delta_{nm} \delta_{AB}(\omega - \Omega_m) - F_m \Lambda_{AB}^{mn}(\mathbf{k})\} = 0. \quad (3)$$

Here A and B are the sublattice indices, $\Lambda(\mathbf{k})$ is the Fourier transform of the intercell interactions, and $F_m = \langle X_{\mathbf{f}}^{n+1, \gamma_1, n+1, \gamma_1} \rangle + \langle X_{\mathbf{f}}^{n, \gamma_2, n, \gamma_2} \rangle$ is the filling factor, which depends on the temperature and hole concentration.

The cell can be divided by various methods. The simplest case of a CuO₂ cell was used to calculate the hole spectrum in the paramagnetic²² and antiferromagnetic phases.²³ However, the more symmetric clusters, CuO₄ or CuO₆, are more convenient because they correctly reflect the local symmetry of copper, but they cannot cover the entire lattice with nonintersecting clusters. Each in-plane oxygen ion belongs directly to two clusters and nonorthogonality of the Hubbard operators arises in neighboring cells. To solve this problem for the three-band p - d model, it was suggested in Refs. 24 and 25 that Wannier functions should be constructed for each cell and then used to determine the X operators. After this procedure, the results of both approaches are almost the same. We shall subsequently use a simpler division into O-Cu-O clusters.

The results of the exact diagonalization of the CuO₆ or CuO₄Cl₂ clusters described above indicate that the singlet-triplet splitting $\Delta\varepsilon_2$ is small ($\Delta\varepsilon_2 < 0.5$ eV), and this will be used subsequently.

For the local basis shown in Fig. 2a, the top of the valence band is determined by three Fermi modes

$$\begin{aligned} X_\sigma^{\alpha_0} &= |1, -\sigma\rangle\langle 2, 0|, & X_\sigma^{\alpha_1} &= |1, -\sigma\rangle\langle 2, 1, 0|, \\ X_\sigma^{\alpha_2} &= |1, -\sigma\rangle\langle 2, 1, 2\sigma|, \end{aligned} \quad (4)$$

where $|1, \sigma\rangle$ is the lowest molecular orbital in the single-hole sector, $|2, 0\rangle$ is the Zhang-Rice singlet, and $|2, 1, M\rangle$, $M=0, \pm 1$ are two-hole triplets. We shall adopt the Zaitsev notation²⁶ in which the initial and final states are replaced by a single root vector $X^{pq} \rightarrow X^\alpha$. The excitation energies (4) in the zeroth approximation are given by

$$\begin{aligned} \Omega_0 &= E(2, 0) - E(1, -\sigma), & \Omega_1 &= E(2, 1, 0) - E(1, -\sigma), \\ \Omega_2 &= E(2, 1, 2\sigma) - E(1, -\sigma). \end{aligned}$$

We use a double-sublattice Fourier transformation to describe the antiferromagnetic phase. Assuming that $X_{\mathbf{k}}^\alpha$ and $Y_{\mathbf{k}}^\alpha$ denote the Fourier transforms of the Hubbard operator in sublattices 1 and 2, the Hamiltonian of an intercluster hop allowing for the Fermi modes (3) has the form

$$\begin{aligned} H_{pd} &= \tilde{T}_{pd} \sum_{\mathbf{k}\sigma} \gamma(\mathbf{k}) X_{\mathbf{k}\sigma}^{+\alpha_0} Y_{\mathbf{k}\sigma}^{\alpha_0} + 2i\sigma(\sin(k_x a) X_{\mathbf{k}\sigma}^{+\alpha_1} Y_{\mathbf{k}\sigma}^{\alpha_0} \\ &\quad + \sin(k_y a) X_{\mathbf{k}\sigma}^{+\alpha_0} Y_{\mathbf{k}\sigma}^{\alpha_1}) + 2i\sigma\sqrt{2}(\sin(k_x a) X_{\mathbf{k}\sigma}^{+\alpha_2} Y_{\mathbf{k}\sigma}^{\alpha_0} \\ &\quad + \sin(k_y a) X_{\mathbf{k}\sigma}^{+\alpha_0} Y_{\mathbf{k}\sigma}^{\alpha_2}) + \text{h.c.}, \end{aligned} \quad (5)$$

where the following notation is introduced

$$\begin{aligned} \gamma(\mathbf{k}) &= \cos(k_x a) + \cos(k_y a), \\ \tilde{T}_{pd} &= -T_{pd}(uv_0 + u_0v)/2, \\ u^2 &= (1 + \delta nu)/2, & v^2 &= 1 - u^2, \\ \delta &= \varepsilon_p - \varepsilon_d, & v^2 &= \delta^2 + 8T_{pd}^2, \\ u_0^2 &= (1 + \delta_0/v_0)/2, & v_0^2 &= 1 - u_0^2, \\ \delta_0 &= \delta - V_{pd}, & v_0^2 &= \delta_0^2 + 8T_{pd}^2. \end{aligned}$$

For typical values of the parameters a renormalized hop is $\tilde{T}_{pd} \approx 0.1$ eV. The first term in Eq. (5) describes a quasiparticle (hole) hop with the excitation of a Zhang-Rice singlet while the second and third terms describe a hole hop with singlet-triplet mixing. The mixing vanishes at the Γ point. Details of calculations of the band structure in the antiferromagnetic phase are given in Ref. 23, and we used this procedure to calculate the hole dispersion law for undoped Sr₂CuO₂Cl₂ (Fig. 3). A comparison between our calculations and the ARPES data shows far better agreement than that obtained for calculations using the t - J model.²⁰ Since the t - J model can only be obtained with a local basis, as in Fig. 2b, where there are no triplet states and singlet-triplet mixing far from the Γ point, we conclude that allowance for the triplet states of two holes and its mixing with the Zhang-Rice singlet are important to describe the hole spectrum in the narrow energy range 0.1–0.5 eV below the top of the valence band, i.e., where high-temperature superconductivity is clearly an important effect.

4. INTERACTION OF HOLES WITH SPIN EXCITONS

Singlet-triplet mixing described by the last two terms in Eq. (5) may result in an additional mechanism of superconducting pairing. These terms resemble interband transitions which may well be a source of pairing.²⁷ These components of H_{pd} may also be explicitly written as Fermion-boson interaction using Hubbard operator algebra, whereby we have

$$X_i^{|2,1,0\rangle(1,-\sigma)} = X_i^{|2,1,0\rangle(2,0)} X_i^{|2,0\rangle(1,-\sigma)}. \quad (6)$$

This implies that the addition of a hole to the initial state $|1, -\sigma\rangle$ with the formation of a final triplet state (the process $|1, -\sigma\rangle \rightarrow |2, 1, 0\rangle$) is equivalent to the generation of a hole in the process $|1, -\sigma\rangle \rightarrow |2, 0\rangle$ with the final state being a Zhang-Rice singlet, and the simultaneous generation of a spin exciton $|2, 0\rangle \rightarrow |2, 1, 0\rangle$. It has been shown that the spin splitting energy $\Delta\varepsilon_2$ is small. Other exciton excitations from the singlet to higher two-hole terms are possible from the point of view of Hubbard operator algebra but are less effective because of the higher energy.

At the same time, the second term in Eq. (5) determines the exchange of spin excitons with $S_z = 0$ without hole spin flipping, which may lead to pairing, and the third term describes the emission and absorption of a spin exciton with $S_z = 1$, i.e., with spin flipping. This may give rise to pairing as in paramagnon exchange, and may also cause pair destruction as a result of hole spin flipping.

Note that this pairing mechanism may occur only in systems doped with holes with nonzero filling of two-hole states.

A multiband p - d model allowing for the $d_{3z^2-r^2}$ orbitals of copper as well as $d_{x^2-y^2}$ orbitals was considered in Ref. 18, where it was shown that an increase in the population of the a_{1g} single-electron molecular orbitals reduces the population of the b_{1g} states and therefore lowers T_c . From our point of view (Figs. 1a and 1b), a substantial increase in the fraction of a_{1g} single-electron orbitals is clear evidence that singlet-triplet crossover may take place in these compounds. The need to allow for the $d_{3z^2-r^2}$ states to obtain an

adequate description of the low-energy part of the electron spectrum of $\text{Sr}_2\text{CuO}_2\text{Cl}_2$ is also noted in Ref. 28 using *ab initio* band calculations and comparing these with the strong coupling model.

We consider it meaningless to write the equations from the Bardeen–Cooper–Schrieffer theory in which the phonon parameters would be replaced by spin-exciton ones, since other mechanisms of superconductivity are also known in this model of the electronic structure: kinematic exchange,²⁹ caused by the first term in Eq. (5), exchange of excitons-crystal-lattice excitations, and paramagnon exchange (see a recent review presented in Ref. 30). In this study we wish to stress that the possibility of spin-exciton pairing in *p*-type copper oxides is caused by the specific characteristics of their electronic structure, specifically the proximity of singlet and triplet current two-hole states.

This work was carried out under the State Program “Superconductivity” (Project No. 93237) and was also supported by the Krasnoyarsk Region Science Foundation (Project No. 5F0009).

¹ V. J. Emery, Phys. Rev. Lett. **58**, 2794 (1987).

² C. M. Varma, S. Schmitt-Rink, and A. E. Ruchenstein, Solid State Commun. **62**, 681 (1987).

³ F. C. Zhang and T. M. Rice, Phys. Rev. B **37**, 3759 (1988).

⁴ E. Dagotto, Rev. Mod. Phys. **66**, 763 (1994).

⁵ A. Kampf, Phys. Rep. **249**, 219 (1994).

⁶ W. Brenig, Phys. Rep. **251**, 153 (1995).

⁷ A. Bianconi *et al.*, Physica C **162–164**, 209 (1990).

⁸ Y. Romberg *et al.*, Phys. Rev. B **41**, 2609 (1990).

⁹ Yu. Gaididev and V. M. Loktev, Phys. Status Solidi B **147**, 307 (1988).

¹⁰ W. Weber, Z. Phys. B **70**, 323 (1988).

¹¹ H. Eskes and G. A. Sawatzky, Phys. Rev. B **44**, 9556 (1991).

¹² H. Eskes, L. H. Tjeng, and G. A. Sawatzky, Phys. Rev. B **41**, 288 (1990).

¹³ H. Kamimura and M. Eto, J. Phys. Soc. Jpn. **59**, 3053 (1990).

¹⁴ S. G. Ovchinnikov and I. S. Sandalov, Physica C **198**, 607 (1989).

¹⁵ V. J. Emery and G. Reiter, Phys. Rev. B **38**, 11 938 (1988); **41**, 7247 (1990).

¹⁶ B. O. Wells *et al.*, Phys. Rev. Lett. **74**, 964 (1995).

¹⁷ V. F. Elesin and V. A. Kashurnikov, Zh. Éksp. Teor. Fiz. **106**, 1773 (1994) [JETP **79**, 961 (1994)].

¹⁸ M. Grilli, C. Castellani, and C. Di Castro, Phys. Rev. B **42**, 6233 (1990).

¹⁹ A. Fujimori, Y. Tokura *et al.*, Phys. Rev. B **40**, 7303 (1989).

²⁰ A. Nazarenko, K. J. E. Vos, S. Haas *et al.*, J. Supercond. **8**, 671 (1995).

²¹ J. C. Hubbard, Proc. Phys. Soc. London, Sect. A **276**, 238 (1963).

²² S. G. Ovchinnikov, Zh. Éksp. Teor. Fiz. **102**, 127 (1992) [Sov. Phys. JETP **75**, 67 (1992)].

²³ S. G. Ovchinnikov, Zh. Éksp. Teor. Fiz. **107**, 726 (1995) [JETP **80**, 451 (1995)].

²⁴ S. V. Lovtsov and V. Yu. Yushankhai, Physica C **179**, 159 (1991).

²⁵ J. H. Jefferson, H. Eskes, and L. F. Feiner, Phys. Rev. B **45**, 7959 (1992).

²⁶ R. O. Zaïtsev, Zh. Éksp. Teor. Fiz. **68**, 207 (1975) [Sov. Phys. JETP **41**, 100 (1975)].

²⁷ B. T. Geïlikman, Usp. Fiz. Nauk. **109**, 65 (1973) [Sov. Phys. Usp. **16**, 17 (1973)].

²⁸ L. F. Mattheiss, Phys. Rev. B **42**, 354 (1990).

²⁹ R. O. Zaïtsev and V. A. Ivanov, Fiz. Tverd. Tela (Leningrad) **29**, 2554 (1987) [Sov. Phys. Solid State **29**, 1475 (1987)].

³⁰ V. N. Loktev, Fiz. Nizk. Temp. **22**, 3 (1996) [Low Temp. Phys. **22**, 1 (1996)].

Translated by R. M. Durham